

## SUPPORTING INFORMATION

### Improvement of Carbon Dioxide Electroreduction by Crystal Surface

#### Modification of ZIF-8

Ting Zhang<sup>a,b†</sup>, Hong Liu<sup>c†</sup>, Xu Han<sup>a</sup>, Martí Biset-Peiró<sup>b</sup>, Yunhui Yang<sup>a</sup>, Inhar Imaz<sup>a</sup>, Daniel Maspoch<sup>a,d</sup>, Bo Yang<sup>c\*</sup>, Joan Ramon Morante<sup>b,e</sup>, Jordi Arbiol<sup>a,d\*</sup>

<sup>a</sup>Catalan Institute of Nanoscience and Nanotechnology (ICN2), CSIC and BIST, Campus UAB, Bellaterra, 08193, Barcelona, Catalonia, Spain

<sup>b</sup>Catalonia Institute for Energy Research (IREC), Jardins de les Dones de Negre 1, Sant Adrià del Besòs, Barcelona 08930, Catalonia, Spain

<sup>c</sup>School of Physical Science and Technology, ShanghaiTech University, 393 Middle Huaxia Road, Shanghai 201210, China

<sup>d</sup>ICREA, Pg. Lluís Companys 23, 08010, Barcelona, Catalonia, Spain

<sup>e</sup>Department of Physics, Universitat de Barcelona, 08028, Barcelona, Catalonia, Spain

\*Corresponding author:

E-mail: yangbo1@shanghaitech.edu.cn, arbiol@icrea.cat

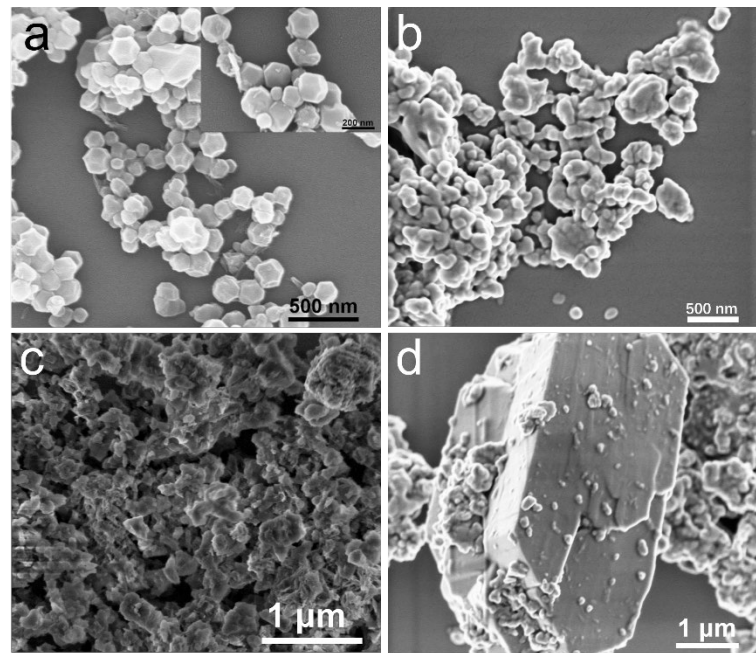


**Fig. S1.** FE-SEM images of (a) ZIF-8-1.7% (b) ZIF-8-10%, (c) ZIF-8-17% and (d) ZIF-8-33%.

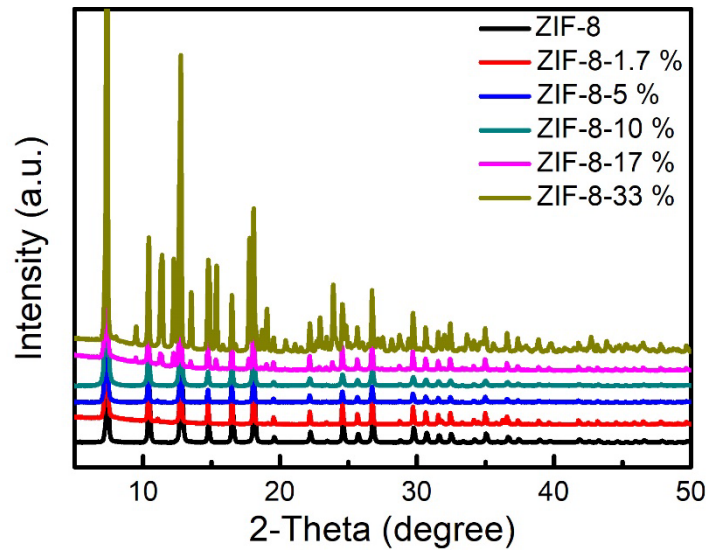


**Fig. S2.** Experimental XRD patterns of ZIF-8 and ZIF-8-x with different DOBDC modification ratios.

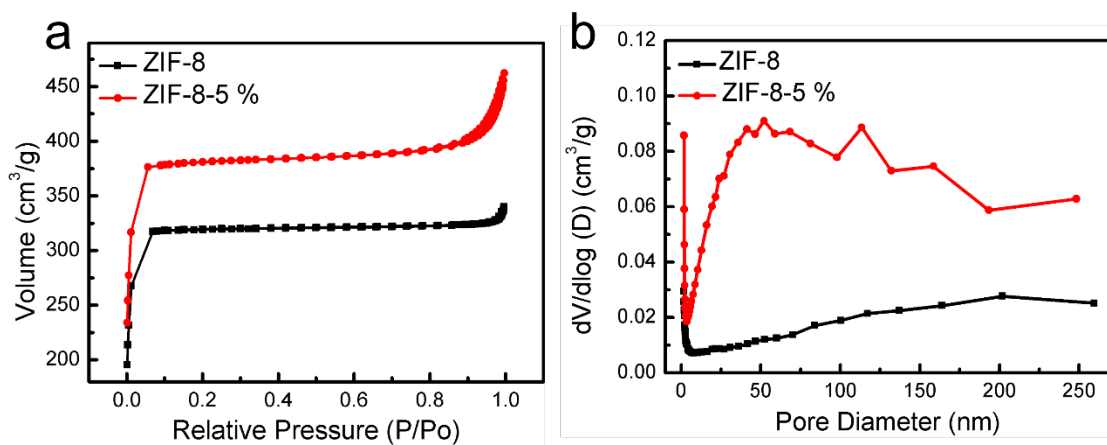


**Fig. S3.** (a) N<sub>2</sub> adsorption-desorption isotherms and (b) corresponding pore size distributions of ZIF-8 and ZIF-8-5% samples.

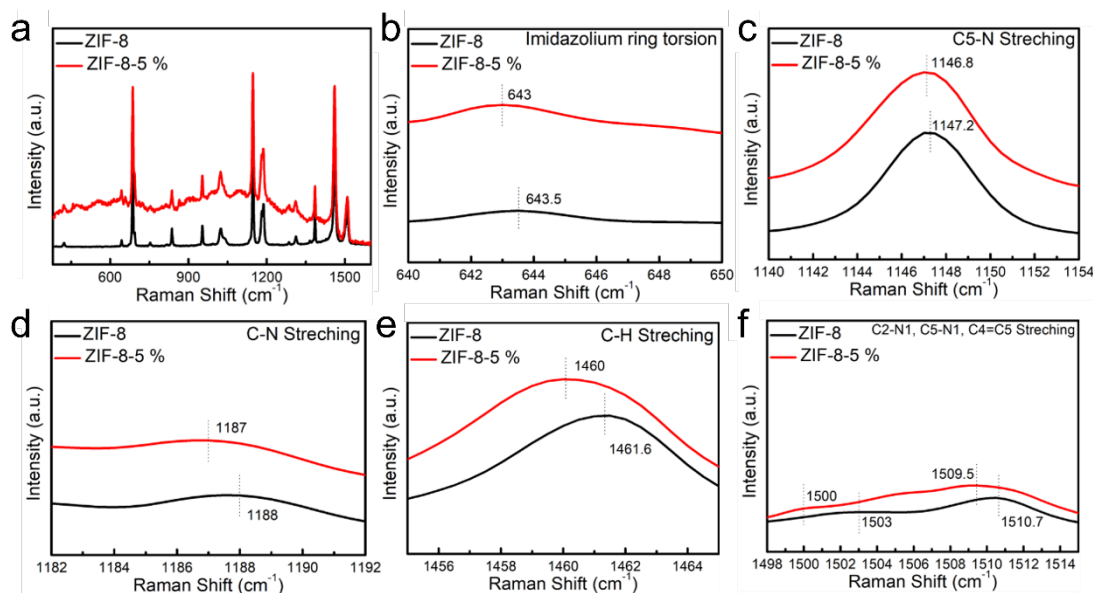


**Fig. S4.** Raman spectra of the ZIF-8 and ZIF-8-5%.

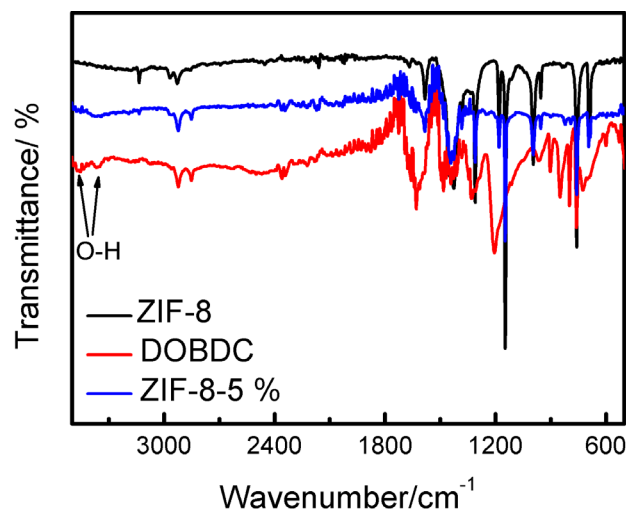


**Fig. S5.** FTIR spectra of the ZIF-8, DOBDC and ZIF-8-5%.

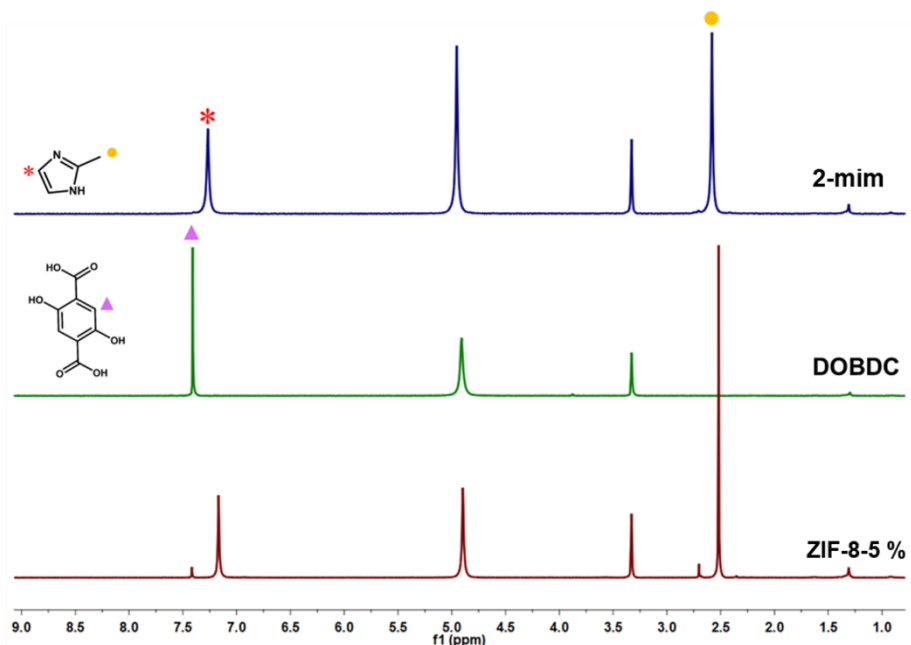


**Fig. S6.** <sup>1</sup>H-NMR spectra of ZIF-8-5 %.

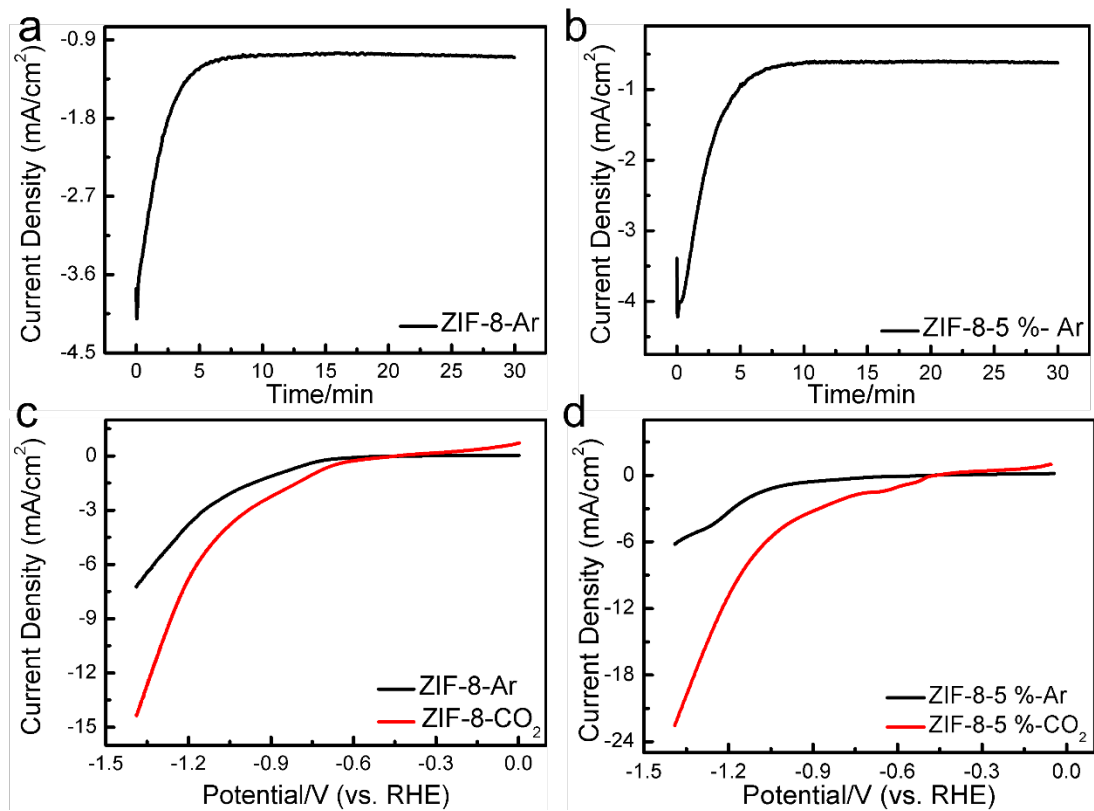


**Fig. S7.** (a and b) Electrode current recorded during reduction of ZIF-8 and ZIF-8-5% at  $-0.90$  V vs. RHE in  $0.5$  M NaHCO<sub>3</sub> purged with Ar; (c and d) LSV curves of ZIF-8 and ZIF-8-5% in Ar- and CO<sub>2</sub>-saturated  $0.5$  M NaHCO<sub>3</sub> solution (scan rate:  $20$  mV/s).

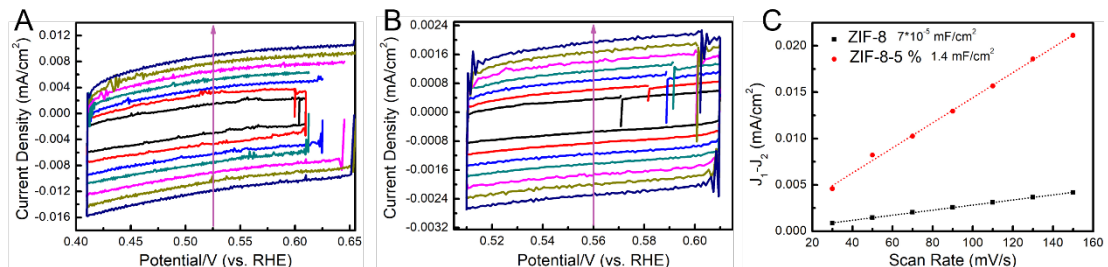


**Fig. S8.** Cyclic voltammograms curves for (a) ZIF-8 and (b) ZIF-8-5%. (c) Plots of the current density vs. scan rate for ZIF-8 and ZIF-8-5% electrodes.

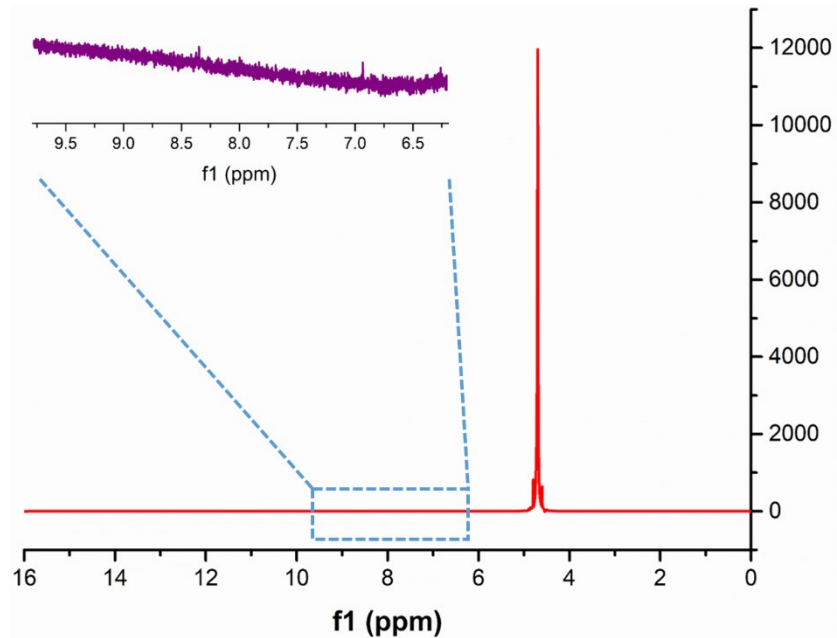


**Fig. S9.** The representative  $^1\text{H}$ -NMR spectra of the electrolyte after electrolysis of  $-1.20$  V for ZIF-8-5% in  $\text{CO}_2$ -saturated  $0.5$  M  $\text{NaHCO}_3$  electrolyte for  $12$  h.

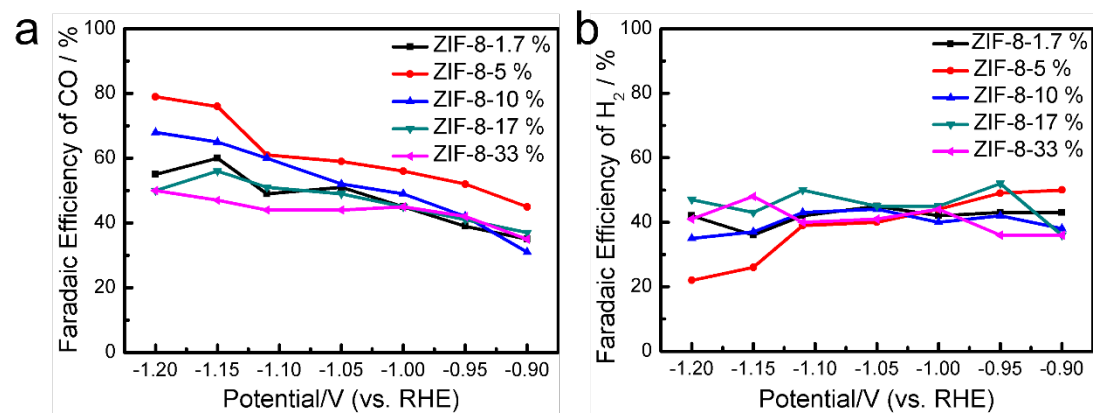


**Fig. S10.** Corresponding FE of (a) CO and (b)  $\text{H}_2$  on ZIF-8-x samples with different modifying ratio.

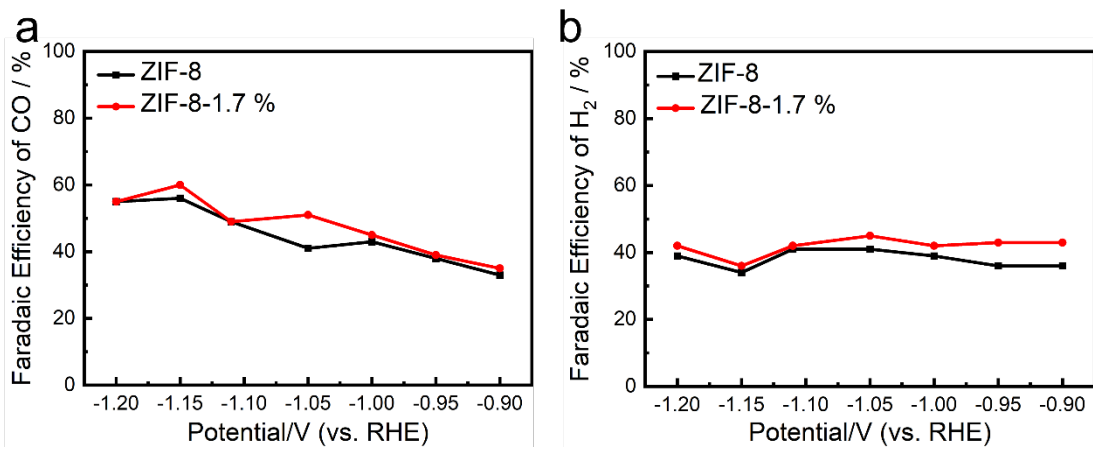


**Fig. S11.** Corresponding FE of (a) CO and (b) H<sub>2</sub> on ZIF-8 and ZIF-8-1.7% samples with different modifying ratio.

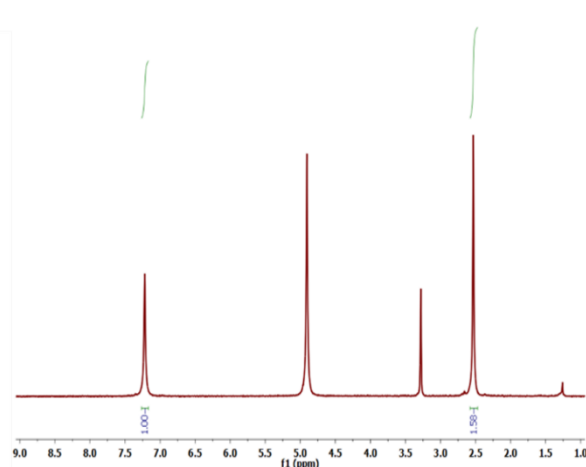


**Fig. S12.** <sup>1</sup>H-NMR spectra of ZIF-8-1.7%.

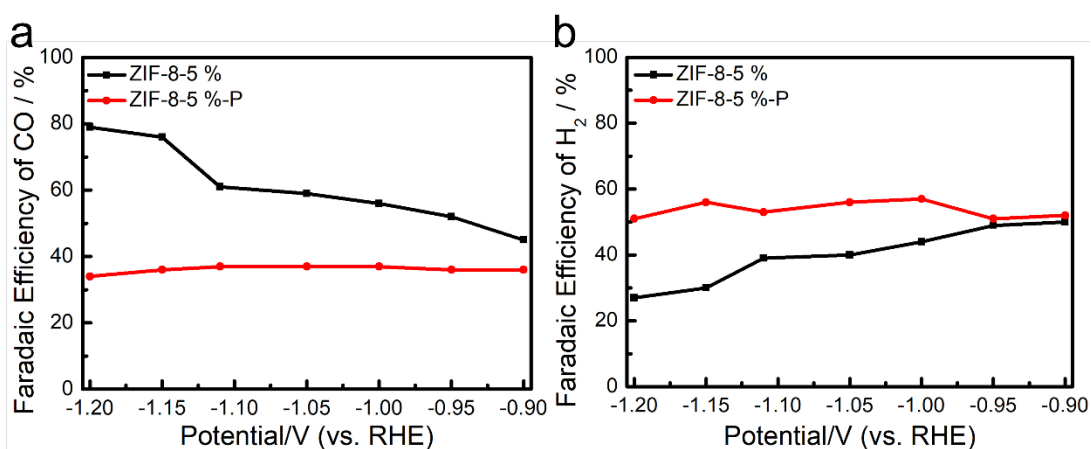


**Fig. S13.** FE of (a) CO and (b) H<sub>2</sub> on ZIF-8-5% and ZIF-8-5%-P electrodes.

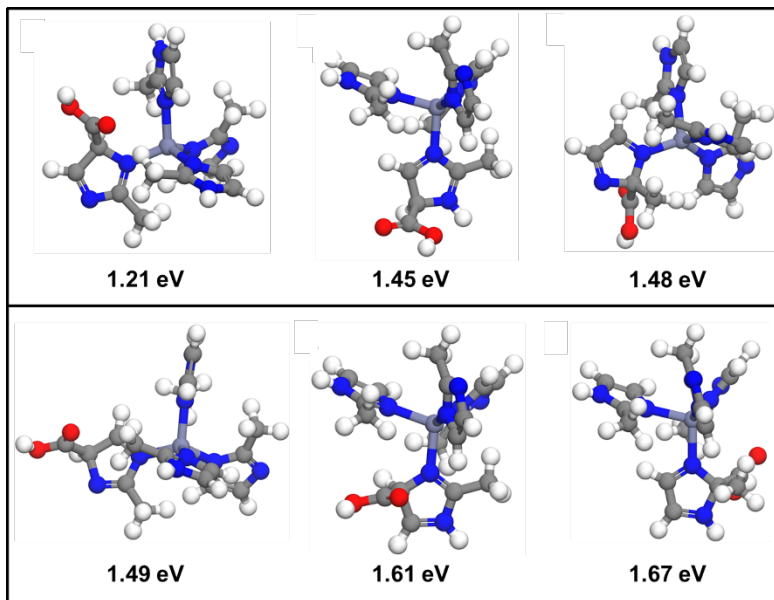


**Fig. S14.** Optimized models of adsorption structure of  $\text{COOH}^*$  and free-energy ( $\text{CO}_2 \rightarrow \text{COOH}^*$ ) on different sites on ZIF-8 (Zn, C, N, O atoms are represented in purple, grey, blue, and red, respectively).

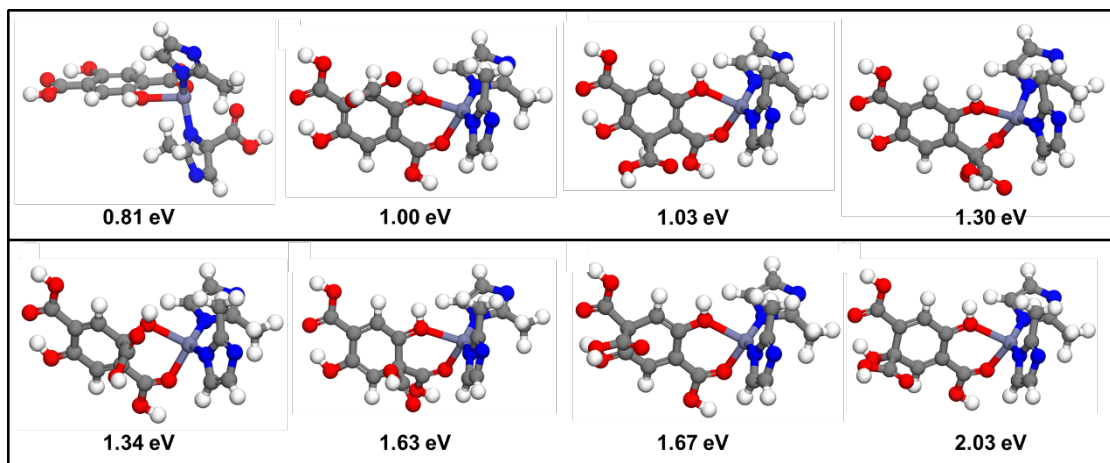


**Fig. S15.** Optimized models of adsorption structure of  $\text{COOH}^*$  free-energy ( $\text{CO}_2 \rightarrow \text{COOH}^*$ ) on different sites on ZIF-8-5% (Zn, C, N, O atoms are represented in purple, grey, blue, and red, respectively).

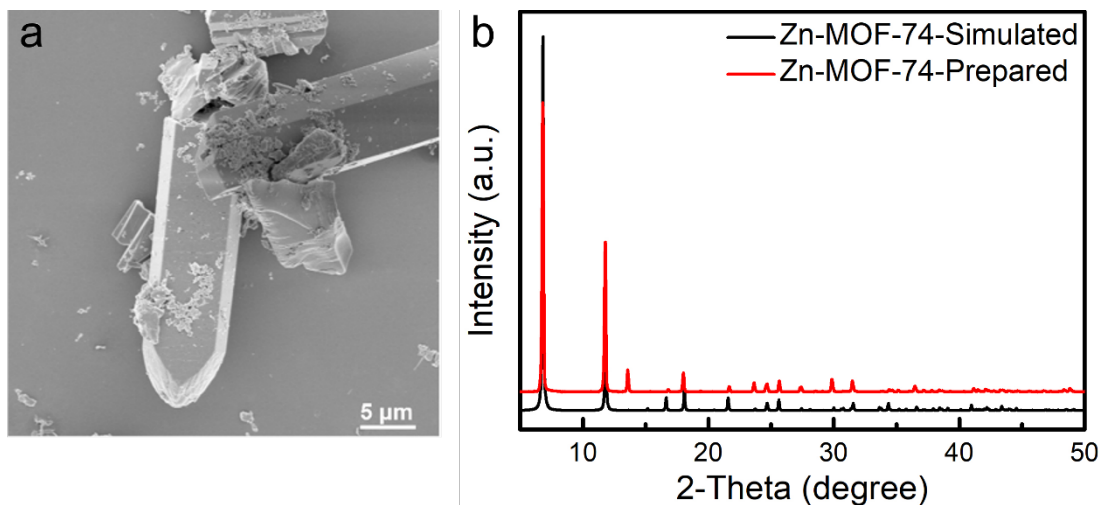


**Fig. S16.** (a) SEM, (b) XRD images of Zn-MOF-74.

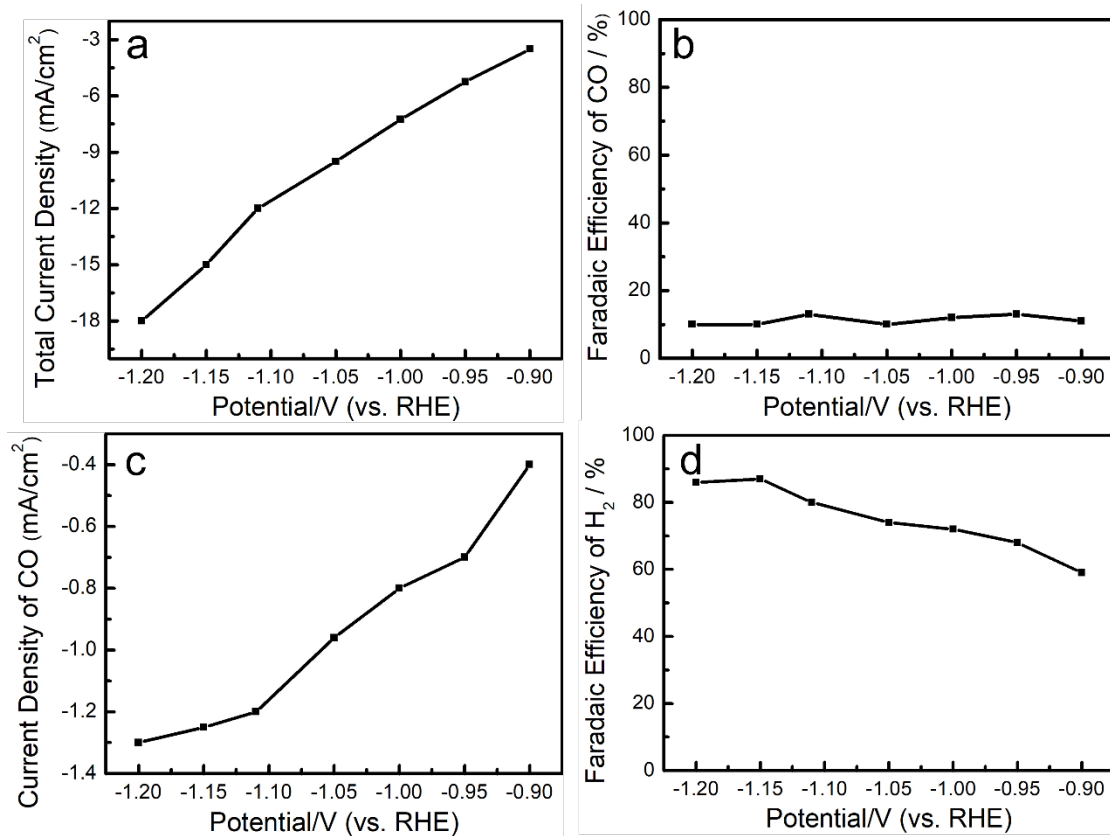


**Fig. S17.** (a) Total current densities for Zn-MOF-74 sample coated on carbon paper in  $\text{CO}_2$ -saturated 0.5 M  $\text{NaHCO}_3$  solution at different applied potentials. (b) Corresponding FE for CO. (c) Partial current densities of CO. (d) Corresponding FE for  $\text{H}_2$ .

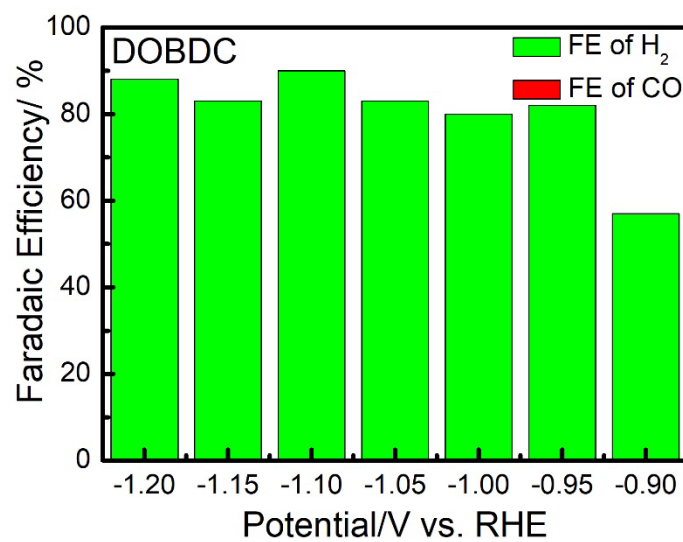


**Fig. S18.** FE of CO and  $\text{H}_2$  on pure DOBDC ligand.

**Table S1.** Faradaic Efficiency of the reported MOFs-based electrocatalysts for CO<sub>2</sub> electroreduction

Catalyst	Electrolyte	Product	FE	Current Density (CO)	Potential	Reference
ZIF-8	0.5 M KHCO <sub>3</sub>	CO	65%	-1.75 mA/cm <sup>2</sup>	-1.8 V vs. SCE	<sup>1</sup>
ZIF-8	0.25 M K <sub>2</sub> SO <sub>4</sub>	CO	81%	-7 mA/cm <sup>2</sup>	-1.1 V vs. RHE	<sup>2</sup>
HKUST-1	0.5 M KHCO <sub>3</sub>	CH <sub>3</sub> OH	5.6%	-10 mA/cm <sup>2</sup>	-1.0 V vs. Ag/AgCl	<sup>3</sup>
HKUST-1	0.5 M KHCO <sub>3</sub>	C <sub>2</sub> H <sub>5</sub> OH	10.3%	-10 mA/cm <sup>2</sup>	-1.0 V vs. Ag/AgCl	<sup>3</sup>
HKUST-1	1 M KOH	C <sub>2</sub> H <sub>4</sub>	45%	262 mA/cm <sup>2</sup>	-1.07 V vs. RHE	<sup>4</sup>
Al <sub>2</sub> (OH) <sub>2</sub> TCPP-Co	0.5 M K <sub>2</sub> CO <sub>3</sub>	CO	76%	-1 mA/cm <sup>2</sup>	-0.7 V vs. RHE	<sup>5</sup>
ZIF-A-LD	0.1 M KHCO <sub>3</sub>	CO	73%	-5 mA/cm <sup>2</sup>	-1.1 V vs. RHE	<sup>6</sup>
ZIF-A-LD/CB	0.1 M KHCO <sub>3</sub>	CO	91%	-7 mA/cm <sup>2</sup>	-1.1 V vs. RHE	<sup>6</sup>
Copper rubeanate MOF	0.5 M KHCO <sub>3</sub>	HCOOH	30%	None	-1.2 V vs. SHE	<sup>7</sup>
Zn-BTC	Ionic liquid	CH <sub>4</sub>	88.3%	0.5 mA/cm <sup>2</sup>	-2.2 V vs. Ag/AgCl	<sup>8</sup>
Cu installed NU-1000	0.1 M NaClO <sub>4</sub>	HCOOH	31%	-1.2 mA/cm <sup>2</sup>	-0.82 V vs. RHE	<sup>9</sup>
MOF-1992	0.1 M KHCO <sub>3</sub>	CO	80 %	-16.5 mA/cm <sup>2</sup>	-0.63 V vs. RHE	<sup>10</sup>
Fe/ZIF-8	0.1 M KHCO <sub>3</sub>	CO	89.1%	-1.8 mA/cm <sup>2</sup>	-0.33 V vs. RHE	<sup>11</sup>
<b>ZIF-8-5 %</b>	<b>0.5 M NaHCO<sub>3</sub></b>	<b>CO</b>	<b>79%</b>	<b>-10 mA/cm<sup>2</sup></b>	<b>-1.2 V vs. RHE</b>	<b>This work</b>

## References

1. Y. Wang, P. Hou, Z. Wang and P. Kang, *ChemPhysChem*, 2017, **18**, 3142-3147.
2. X. Jiang, H. Li, J. Xiao, D. Gao, R. Si, F. Yang, Y. Li, G. Wang and X. Bao, *Nano Energy*, 2018, **52**, 345-350.
3. J. Albo, D. Vallejo, G. Beobide, O. Castillo, P. Castaño and A. Irabien, *ChemSusChem*, 2017, **10**, 1100-1109.
4. D.-H. Nam, O. S. Bushuyev, J. Li, P. De Luna, A. Seifitokaldani, C.-T. Dinh, F. P. García de Arquer, Y. Wang, Z. Liang, A. H. Proppe, C. S. Tan, P. Todorović, O. Shekhah, C. M. Gabardo, J. W. Jo, J. Choi, M.-J. Choi, S.-W. Baek, J. Kim, D. Sinton, S. O. Kelley, M. Eddaoudi and E. H. Sargent, *J. Am. Chem. Soc.*, 2018, **140**, 11378-11386.
5. N. Kornienko, Y. Zhao, C. S. Kley, C. Zhu, D. Kim, S. Lin, C. J. Chang, O. M. Yaghi and P. Yang, *J. Am. Chem. Soc.*, 2015, **137**, 14129-14135.
6. S. Dou, J. Song, S. Xi, Y. Du, J. Wang, Z.-F. Huang, Z. J. Xu and X. Wang, *Angew. Chem. Int. Ed.*, 2019, **58**, 4041-4045.
7. R. Hinogami, S. Yotsuhashi, M. Deguchi, Y. Zenitani, H. Hashiba and Y. Yamada, *ECS Electrochem. Lett.*, 2012, **1**, H17-H19.
8. X. Kang, Q. Zhu, X. Sun, J. Hu, J. Zhang, Z. Liu and B. Han, *Chem. Sci.*, 2016, **7**, 266-273.
9. C.-W. Kung, C. O. Audu, A. W. Peters, H. Noh, O. K. Farha and J. T. Hupp, *ACS Energy Lett.*, 2017, **2**, 2394-2401.
10. R. Matheu, E. Gutierrez-Puebla, M. Á. Monge, C. S. Diercks, J. Kang, M. S. Prévot, X. Pei, N. Hanikel, B. Zhang, P. Yang and O. M. Yaghi, *J. Am. Chem. Soc.*, 2019, **141**, 17081-17085.
11. Y. Ye, F. Cai, H. Li, H. Wu, G. Wang, Y. Li, S. Miao, S. Xie, R. Si, J. Wang and X. Bao, *Nano Energy*, 2017, **38**, 281-289.